Hindawi
Advances in Polymer Technology
Volume 2022, Article ID 7448575, 16 pages
https://doi.org/10.1155/2022/7448575

Research Article

Oil-Incorporated Poly(Lactic Acid) as an Alternative Material for Orthodontic Base Plate: A 3D Printing Approach

Niha Naveed,[1] **Kingshuk Dutta**,[2] **D. Balamurugan**,[2] **Amruth V. Haveri**,[2] **and Kannan Sabapathy**[1]

[1]*Department of Orthodontics and Dentofacial Orthopedics, Sree Balaji Dental College and Hospital, Chennai 600100, India*
[2]*Advanced Polymer Design and Development Research Laboratory (APDDRL), School for Advanced Research in Petrochemicals (SARP), Central Institute of Petrochemicals Engineering and Technology (CIPET), Bengaluru 562149, India*

Correspondence should be addressed to Kingshuk Dutta; kingshukdutta.pst@gmail.com

Received 31 March 2022; Accepted 5 August 2022; Published 25 August 2022

Academic Editor: Leonard D. Tijing

Removable orthodontic appliances fabricated from poly (methyl methacrylate) (PMMA) have been routinely used for active orthodontic correction and as retention appliances. This article reports the use of a combination of biodegradable-grade poly (lactic acid) (PLA) and cooking-grade sesame oil as a biodegradable alternative for PMMA. The underlying purpose is to combat the environmental hazards due to nondegradable PMMA as well as to overcome its structural and mechanical drawbacks. The fabrication technique that has been used is fused deposition modeling-based 3D printing technology. Oil-dipping for 24 h was done to render the PLA hydrophobic and to reduce its brittleness. Incorporation of oil within the PLA base plate has been confirmed by FT-IR and FT-Raman spectroscopic techniques. The PLA-cooking oil material has exhibited satisfactory tensile, compressive and flexural strengths. The proposed material has demonstrated excellent attributes in terms of product precision, dimensional stability, density, hardness, and maximum load bearing capacity for the purpose of fabricating orthodontic appliances.

1. Introduction

Acrylic-based polymers have been utilized to fabricate various orthodontic appliances for over a century. One such polymer is poly(methyl methacrylate) (PMMA), which became a very popular choice due to its versatility, reliability, and most importantly, biocompatibility. PMMA has been used for a wide range of applications, such as obturators in newborns with congenital defects, space maintainer appliances for children in the mixed dentition period, dentures for patients with missing teeth, prosthesis for various craniofacial defects (such as ocular, nasal, and auditory prostheses), functional appliances for growth modification in growing children, splints to correct temporomandibular joint disorders, active orthodontic appliances to bring about tooth movement, and orthodontic retainers [1]. Until date, acrylic resin based on poly(methyl methacrylate) remains as the state-of-the-art material for fabrication of orthodontic base plates (OBPs) [2–5]. However, it suffers from certain drawbacks; the most important of which is the presence of residual monomer and initiator within the final product [6–9]. These, in turn, get gradually released during the service life of the OBP and may cause health issues within the patients subjected to long-term exposure. Most importantly, PMMA is nonbiodegradable and, thus, causes damage to the environment after the OBPs get discarded after their service life. In addition, although the fabrication of PMMA-based OBPs is simple and quick, the products formed have structural defects, dimensional imperfections, and nonuniformity, causing unwanted variations in their final physical and mechanical properties (Figure S1). For example, in a single PMMA-based OBP, the thickness variation was found to be >2.5 mm, with the lowest and highest

thickness values being 1.9 mm and 4.5 mm, respectively. This range of variation was found to be true for all the base plates pictured in Figure S1.

Pollution caused by plastic materials, especially the single-use plastics, is a very serious problem that is affecting the entire world. These plastic materials take a very long amount of time to degrade or decompose under natural conditions, ranging from decades to centuries and even longer at times. As a result of this long timeframe, the discarded materials cause nuisance to the environment and most often disturb the local ecosystem. One way to reduce the impact of plastic pollution is to recycle the plastic products after their service life. However, recycling has its own limitation. Firstly, the recycled material almost never matches the properties of the original virgin materials, leading to deterioration of the product quality or use in another product of lesser property demand. Secondly, there is a limit to the number of times a material can be recycled. Therefore, after a certain number of recycling cycle, the material has to be eventually discarded or used in purposes such as laying of roads and landfill. Keeping the above aspects in view, the best way forward is to use biodegradable plastic, in the first place, to fabricate the original product. This will ensure that there is no need to worry about the fate of the material after the service life, as it will get biodegraded and mixed with the soil. This is especially applicable for products using single-use plastic materials. PMMA-based OBPs serve as one such single-use plastic. Therefore, it is of great interest to use a biodegradable alternative to PMMA, so that the polluting effect can be prevented.

This work was aimed at developing a biodegradable and biocompatible OBP to replace the state-of-the-art nonbiodegradable PMMA resin-based OBPs. However, this was a challenging task as this was probably the first-of-its-kind approach to replace the well-known and highly suitable PMMA by a biodegradable polymer for fabrication of an OBP. In this research, a combination of biodegradable-grade poly(lactic acid) and cooking-grade sesame oil material was used as a potential replacement of PMMA for the fabrication of OBP. The choice of PLA and sesame oil has been done based on the fact that these are known to be biodegradable, biocompatible, and food contact-safe [10–13]. Also, PLA is one of the most commercially used biopolymers at present and has found use in biomedical applications [14, 15]. In addition, the new-age 3D scanning and printing technology, belonging to the versatile additive manufacturing process [16, 17], has been utilized in this work for the designing and fabrication of the developed OBP. The tests carried out for determining the suitability and applicability of the developed alternative OBP material are water uptake, water swelling degree, saliva uptake, and saliva swelling degree at different temperatures (i.e., 40°C, 90°C, and 0°C) and at different pH (i.e., 5, 7, and 9), FT-IR and FT-Raman, maximum load bearing capacity, surface hardness, density, and tensile, flexural, and compressive strengths. Moreover, the product was found to be odorless and tasteless and is nontoxic to humans as per the information available in the literature [13, 18].

2. Materials and Methods

2.1. Materials. 3D printed filament of PLA was purchased from WANHAO (Mumbai, India). The vacuum-packed filament used was of an average diameter of 1.5 mm and was translucent. Biodegradable grade of PLA was used for this research. Sesame oil used was of cooking grade and was purchased from KLF. Tetrahydrofuran (THF, >99.5% pure grade) was bought from SRL Chemicals (Chennai, India). Artificial saliva (purity: >99.9%) solution was procured from Nanochemazone (Mohali, India). All the chemicals were used as received. Distilled drinking quality water was used for all water dipping purposes.

2.2. Instruments and Software. 3D scanning was performed using Breuckmann Smart Scan 3D 2275 White Light 3D Scanner; while, the 3D printing was done with TECHB Fused Deposition Modeling (FDM) 3D Printer. Geomagic software (2020-21 version) was used for 3D scanning and designing of the product. For structural characterizations and confirmation of the incorporation of oil within the polymer structure, as well as to verify the absence of chemical interactions between the polymer and the oil, Jasco FT/IR-4700 FT-IR spectrophotometer and Thermo Scientific NICOLET iS50 FT-Raman spectrophotometer were used. Compressive, tensile, and flexural strength analyses of the material used were performed with DAK UTB-9103 instrument (ASTM D695, ASTM D638, and ASTM D790, respectively). Maximum load bearing capacity analyses of the OBPs were also performed using DAK UTB-9103 instrument. Density analysis was done using AXIS ALN220G instrument (ASTM D792), and Shore D hardness was measured by Hildebrand Hardness Tester (ASTM D2240). Water absorption analyses were done following ASTM D 570 standard. The majority of characterizations of PMMA- and PLA-based OBPs and their property comparisons have been performed by subjecting them to treatment under identical conditions in the authors' laboratory. This has ensured better comparison, as against comparison with the reported values in the literature. This is because the analyses reported in the literature are not essentially performed under the conditions that have been maintained in the authors' laboratory. However, in cases where direct comparisons in the laboratory were not possible, comparisons have been made with standard reported values. Moreover, all the tests have been performed in triplicate, and the average values have been reported. Percentage deviations have also been indicated, wherever necessary and relevant, for better realization.

2.3. 3D Scanning and 3D Printing Procedures for Fabrication of PLA-Based OBPs. A commercial PMMA-based OBP was first scanned using 3D technique (this can be replaced by scanning of the positive impressions of patients' dental structure that are normally made for fabrication of commercial OBPs). The scan obtained was further designed in order to minimize the product defects and impart uniformity to the product dimension. This design STL file was then made print-ready by converting it to GCODE format by using Ultimaker Cura software. The FDM-based 3D printing of

the PLA OBP was then executed by using a 0.4 mm extrusion nozzle on a flat glass plate. The layer resolution used for printing was 60 μm. The temperature of the nozzle was set at 210°C, while the bed temperature was set at 70°C. For printing, PLA filaments, having an average diameter of 1.5 mm, was used. Although commercially available PLA filaments have been used for this research, it should be noted that this filament can also be fabricated from PLA beads by using the extrusion technique.

2.4. Modification of the 3D Printed PLA OBP by Incorporation of Sesame Oil. The obtained PLA OBP was then dipped in oil for 24 h to allow for requisite uptake of oil by the OBP. The uptake of oil was found to be between 1 to 2 wt% (in this study, this minimal amount has been found to be enough to enhance certain properties of PLA that was essential for it getting fabricated into an OBP). Then, the product was cleaned for excess unabsorbed oil present on the surface. The wire components were then attached onto the PLA-oil OBP by using either PLA melt or highly viscous solution of PLA (in THF). Also, the design of the OBP can be done in such a way to provide provision for insertion of the wires, followed by plugging of the wire holes by PLA melt or highly viscous solution of PLA (in THF).

A schematic of the overall methodology adopted in this work for fabrication and characterization of oil-incorporated PLA OBPs has been presented in Figure 1.

3. Results and Discussion

3.1. 3D Scan, Design, and 3D Print. The 3D scan model that was used for this work has been presented in Figure S2. Based on this model design file, the 3D printing was performed. The obtained 3D printed product, before and after the attachment of the wire component, has been shown in Figure 2. The product obtained is characterized by (a) possession of high level of precision, in terms of uniform weight (detailed in the next section) and uniform thickness (1.75 ± 0.2 mm), and (b) devoid of structural defects and dimensional imperfections. It is to be noted here that an optimized thickness value of 1.75 mm was used because 1.5 mm thick product failed to perform satisfactorily in terms of mechanical properties, while the performance (in terms of essential OBP properties) of the 1.75 mm thick product was either found to be sufficient or almost similar to that achieved for the 2 mm thick product. Therefore, the thickness of 1.75 mm was chosen as the final optimized thickness of the product in order to optimize between the amount of material used and property achievement. The smoothness of the product texture (depicted in Figure 2) can be further enhanced by executing longer smoothening with sandpaper/other relevant tools, or simply by polishing.

3.2. Product Comparison and Product Precision. For any method to be successful, it is very important that the method gives rise to replicated results. In the present case, this means that the 3D printing product, under identical conditions of fabrication, should possess uniform properties. These aspects have been analyzed and presented in this and subsequent sections.

However, before going into the precision analysis, it is more critical to understand the comparison between the PMMA- and PLA-based OBPs, having identical designs and product scale. As already noted above, the PMMA-based OBP model (that has been used in this study for designing the PLA-based OBP) possesses highly varied thickness (i.e., 1.9 mm to 4.5 mm) (Figure S1a and b), whereas the developed PLA-based OBP possesses a uniform 1.75 ± 0.2 mm thickness. Again, in terms of weight of the product, Figure 3(a) clearly shows that the developed OBP is much lighter compared to the commercial product. The obtained results are very significant as a lighter product is likely to be more patient-friendly, and a uniform product will possess better mechanical attributes that shall lead to higher operational life (less chance of failure/breakage) of the product.

Now, coming back to the product precision, it was found that out of the five 3D printed PLA OBPs that were prepared using identical design and fabrication procedure (products 1, 2, 3, 4, and 5), the weight variation was only 0.0109 g (Figure 3(b)). This variation, after uptake of oil, became 0.045 g (Figure 3(b)). The increase in the weight variation after oil-loading can be attributed to the different extent of oil consumed by different PLA OBPs, owing to the minor variation of pores present in the printed products. Nevertheless, this level of product precision, arising out of 3D printing technology, can never be achieved in conventionally prepared PMMA-based OBPs.

3.3. FT-IR and FT-Raman Analyses. FT-IR and FT-Raman analyses were performed in order to verify (a) the purity of PLA and sesame oil used, (b) the incorporation of oil within PLA, and (c) that there is no chemical reaction between the oil and PLA. It must be noted here that the oil was added to reduce the water uptake and brittleness of PLA. In essence, the intended functions of oil were to behave as a plasticizer and as a hydrophobic barrier to water.

In Figure 4(a), the three small peaks appearing at 2994.91 cm^{-1}, 2945.73 cm^{-1}, and 2880.17 cm^{-1} were due to C-H bond stretching frequencies, where the C-atom was sp^3 hybridized. Upon polymerization of the monomer lactic acid to PLA, the carboxylic acid groups present in the monomer gets converted to ester groups. The carbonyl C=O stretching frequency of this ester group appeared at 1747.19 cm^{-1}. On the other hand, the in-chain C-O stretching frequencies were observed at 1452.14 cm^{-1} and 1359.57 cm^{-1}. Again, the bending vibration frequency of the O-C=O present in the ester groups can be observed at 1078.98 cm^{-1}. The peak at 1042.34 cm^{-1} can be attributed to the O-H bending vibration frequency, present in the terminal -OH groups. Hence, it can be safely said, from the detailed analysis of the characteristic peaks that appeared in the FT-IR spectrum of 3D printed PLA, that the PLA used for the fabrication of the OBP is highly pure, as the spectrum did not reflect the presence of any major contaminant(s) [19].

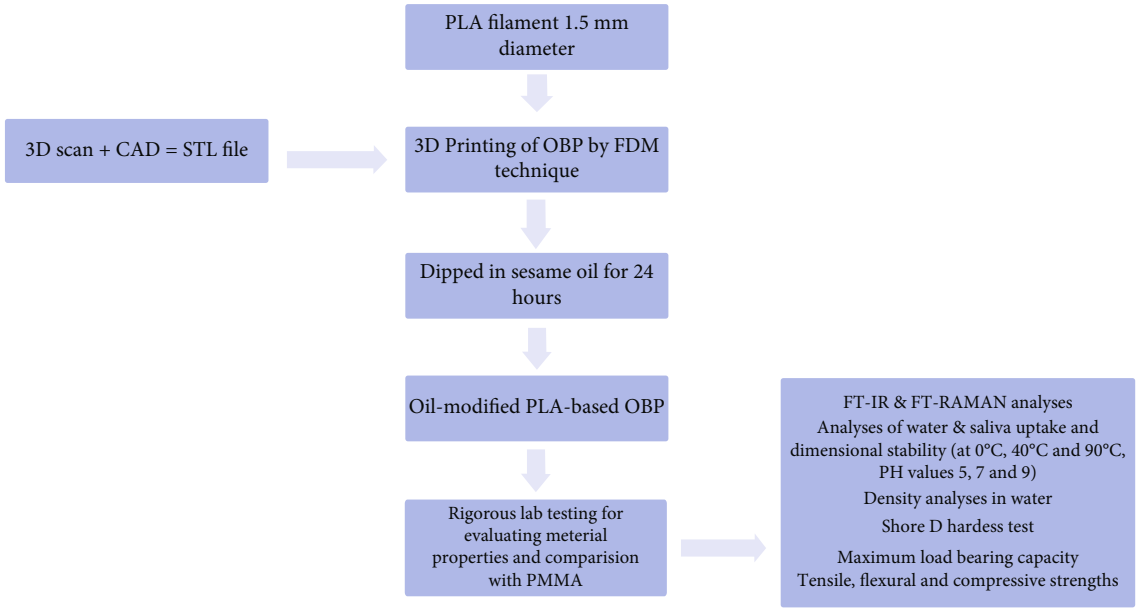

Figure 1: A schematic of the overall methodology adopted for fabrication and characterization of oil-incorporated PLA OBPs.

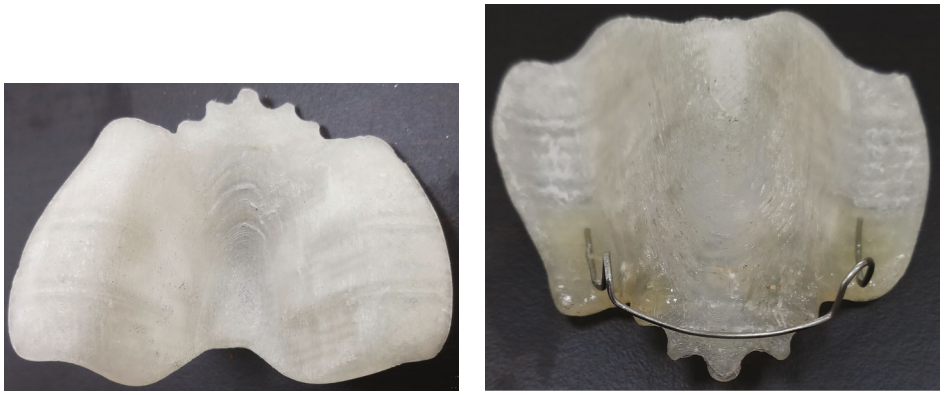

(a) (b)

Figure 2: 3D printed PLA-based OBP (a), with attached wire component (b).

In Figure 4(b), the peaks appearing at 3007.02 cm^{-1} and 2924.09 cm^{-1} were due to sp^3 hybridized C-H stretching frequencies, while the sp^2 hybridized C-H stretching frequency appeared at 2854.65 cm^{-1}. The presence of carboxylic acid groups in sesame oil was confirmed from the peaks observed at 1743.65 cm^{-1} (for carbonyl C=O stretching frequency) and 1458.18 cm^{-1} and 1371.39 cm^{-1} (both for C-O stretching frequencies in carboxylic acid). The bending vibration frequency of O-C=O was observed at 1159.22 cm^{-1}, while the peak corresponding to the O-H bending frequency appeared at 1101.35 cm^{-1}. Hence, the detailed analyses of the characteristic peaks confirmed that the oil used for this study was sesame oil [20], which is comprised majorly of linoleic acid, oleic acid, palmitic acid, and stearic acid. Therefore, this oil is composed of fatty acids that are monounsaturated and polyunsaturated as well as saturated.

Figure 4(c) clearly demonstrates the incorporation of sesame oil within the physical structure of PLA, by physisorption. This is demonstrated by the absence of any major peak shifts in the spectrum of the oil-incorporated PLA OBP, as compared to the individual spectrum of PLA and sesame oil. It is to be noted here that any occurrence of chemical reactions, leading to breakage of existing chemical bonds and generation of new chemical bonds, would have got reflected in the IR spectrum of the oil-incorporated PLA. Moreover, the observed increase in the intensity of the carbonyl C=O peak in the oil-incorporated PLA was due to the increase in the number of such groups after incorporation of oil.

To complement the observations made in the FT-IR analyses, the FT-Raman analyses were performed. It can be clearly seen from the comparative Raman spectra in Figure 5 that the peaks belonging to the individual spectrum of PLA [21] and sesame oil [22] are all present in the spectrum of oil-incorporated PLA. Therefore, the successful incorporation of oil within the structure of PLA, via physisorption, can be undoubtedly realized.

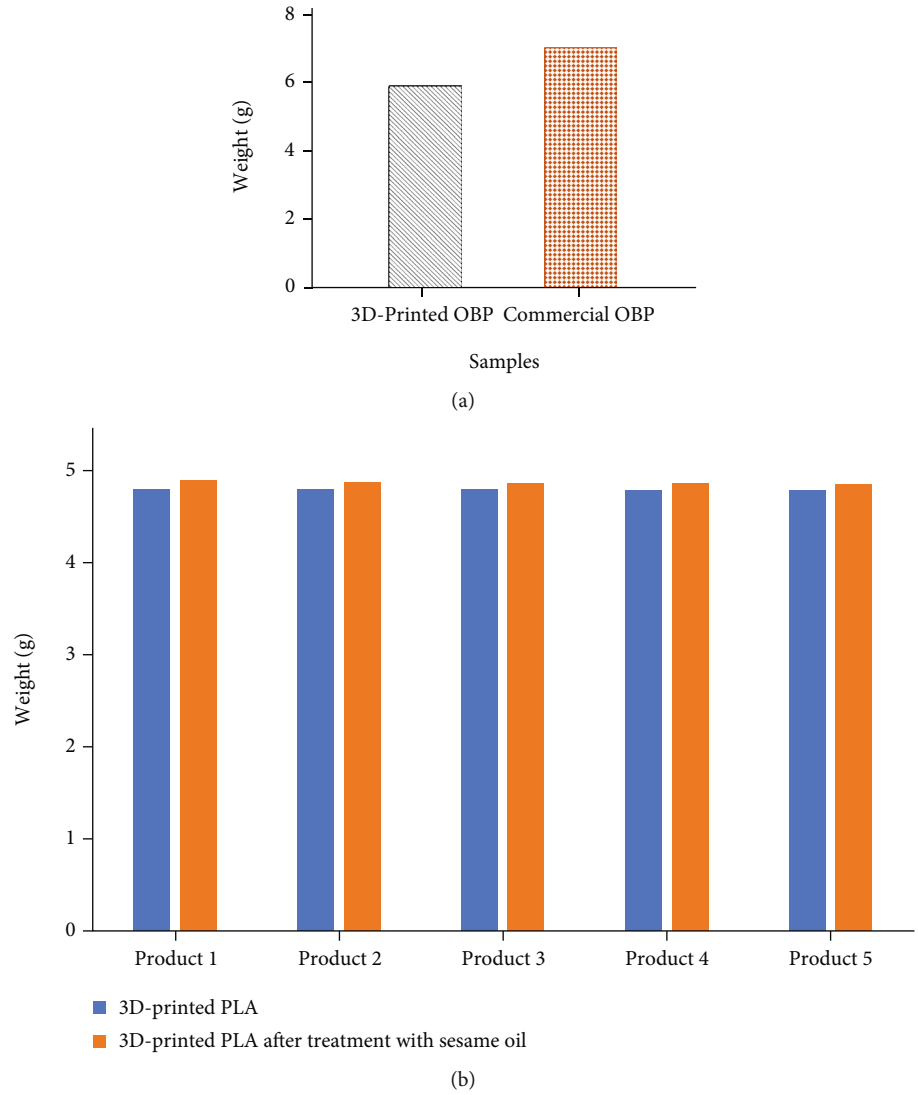

Figure 3: (a) Comparative analysis of the weight of the final OBPs, having same design and scale (standard deviation for 3D printed OBP is ±0.005, standard deviation for commercial OBP is ±0.5) and (b) precision analysis of the untreated and sesame oil-treated 3D printed OBPs.

3.4. Analyses of Water Uptake and Dimensional Stability. Determination of water uptake capacity of an OBP is extremely crucial, as this product has to operate in an aqueous environment. In addition, this product has to face temperature and pH variations (depending upon the nature of food or drink that a patient normally intakes). Therefore, resistance of this product towards these variations must be ensured. For this purpose, water uptake capacity analyses were performed at three different temperatures (i.e., 0°C, 40°C, and 90°C), maintaining the pH value at 7, and two pH values (i.e., 5 and 9) at the abovementioned three temperatures. These ranges of temperature and pH have been selected because majority of the food or drink that human consumes falls within this range.

PLA is known to exhibit moderate water uptake [23]. Analyses at 40°C (at pH 7) for a period of 10 weeks revealed that the oil-modified 3D printed PLA OBP demonstrated much lower water uptake capacities compared to the commercial and unmodified 3D printed PLA OBP (Figures 6(a) and 6(b)). This can be attributed to the presence of oil that resisted the flow of water within the porous structure of PLA. On the other hand, the unmodified 3D printed PLA OBP possessed a porous structure that led to its demonstration of higher water uptake compared to the commercial OBP (Figure 6(b)). This higher porosity is also one of the reasons behind achieving a lower weight product (although the density of PLA is higher than PMMA) in the case of 3D printed OBP, compared to the commercial OBP. From Figure 6(b), it was further realized that the oil-modified PLA OBP showed an initial uptake of water in the first week, followed by no further uptakes. In the unmodified PLA OBP, the uptake took place for the first 2 weeks, followed by no further uptakes. However, in the commercial OBP, the uptake took place for the first 6 weeks, followed by saturation.

Similar to that observed at 40°C, the oil-modified PLA OBP demonstrated the least water uptake at 90°C (at pH 7) due to the reason already explained above (Figures 6(c)

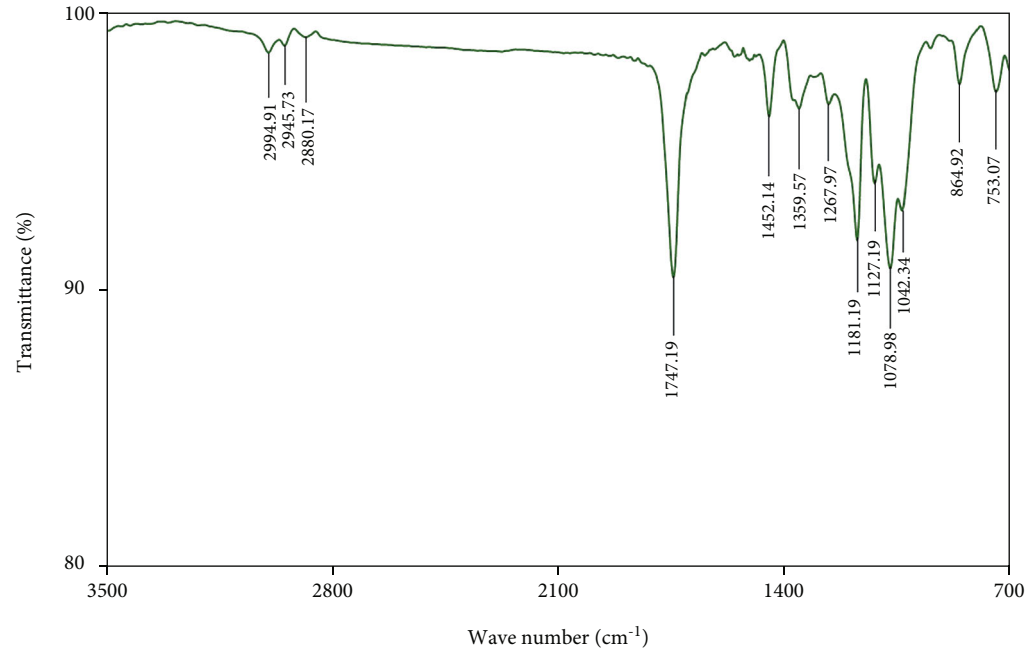

(a)

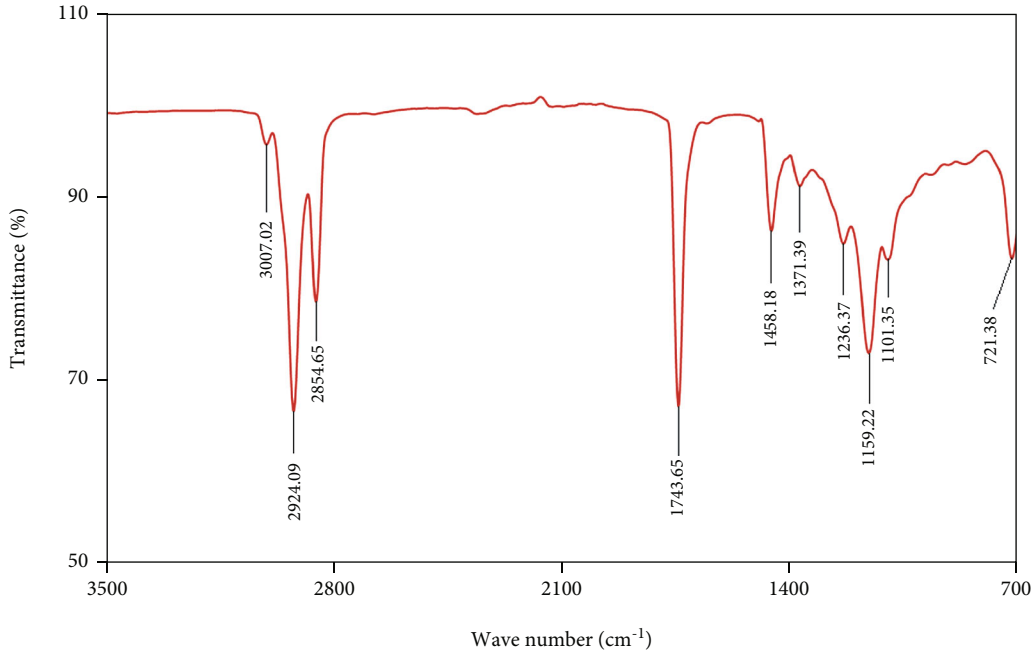

(b)

Figure 4: Continued.

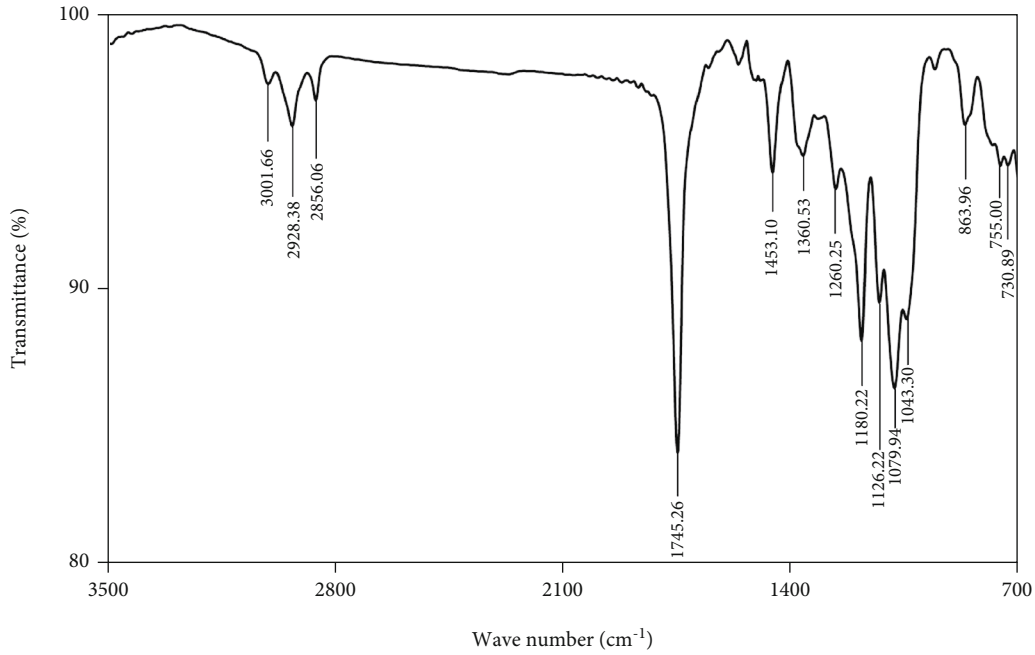

Figure 4: FT-IR spectrum of (a) 3D printed PLA OBP, (b) sesame oil, and (c) sesame oil-treated 3D printed PLA OBP.

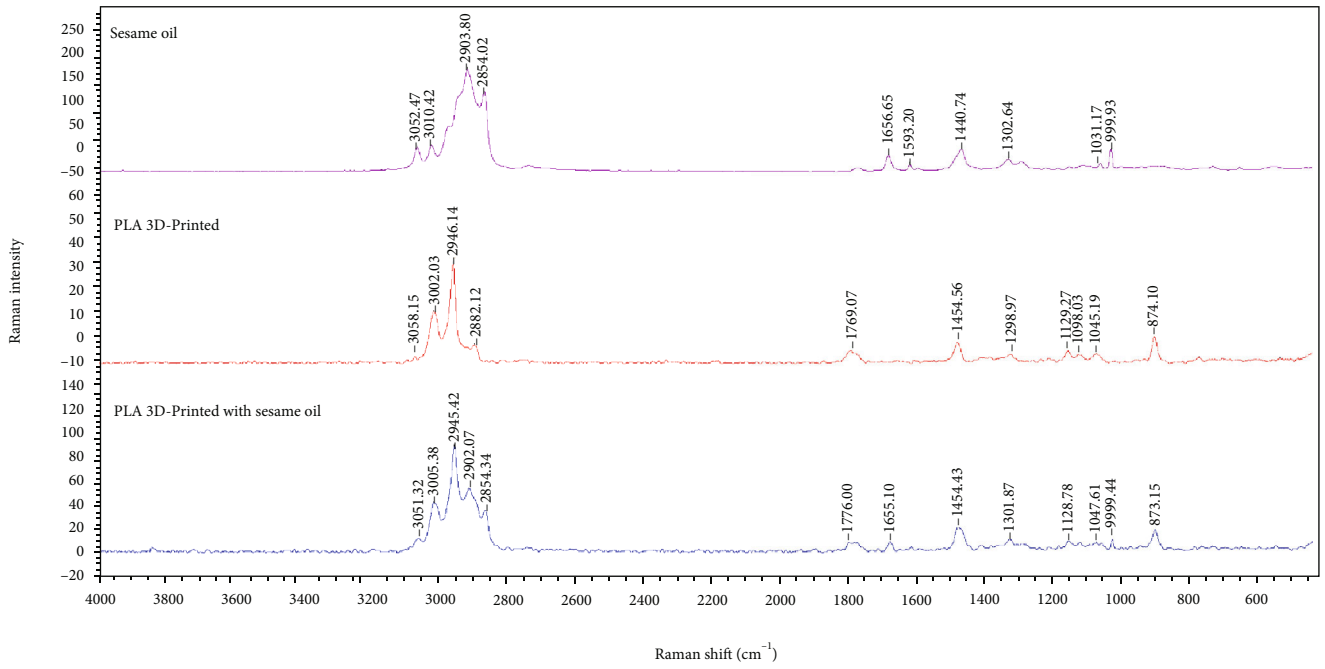

Figure 5: Comparative analysis of the FT-Raman spectra and confirmation of the presence of sesame oil in the final OBP.

and 6(d)). However, contrary to that observed at 40°C, the commercial OBP exhibited a higher water uptake compared to the unmodified PLA OBP at 90°C (Figure 6(d)). This is because, at a higher temperature of 90°C (which is close to the boiling temperature of water), the water molecules were at a much higher kinetic energy state that led to higher Brownian motion. As a result, the distance between two water molecules became longer, leading to decrease in the density. A combined effect of lower density and higher molecular motion led to an overall decrease in the water uptake capacities. It is to be noted here that the extent of porosity had negligible role in influencing the water uptake capacity at 90°C.

At 0°C, the water uptake by any of the OBPs was observed to be nonexistent. This is probably because, at a low temperature of 0°C, the water molecules were much

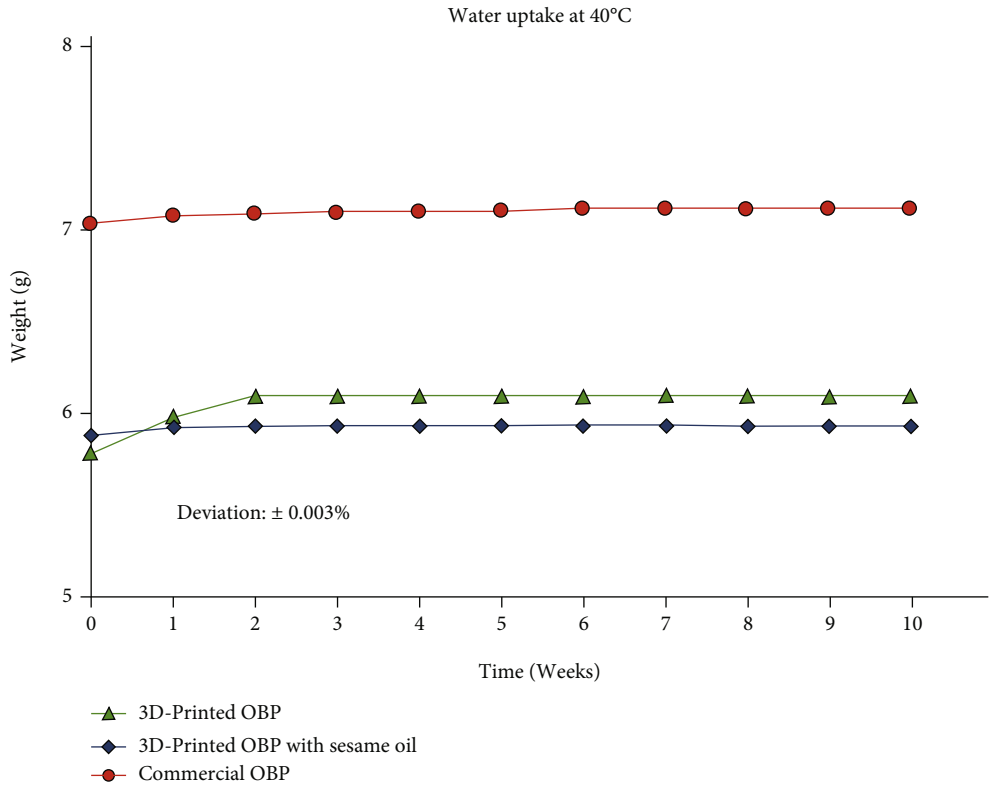

(a)

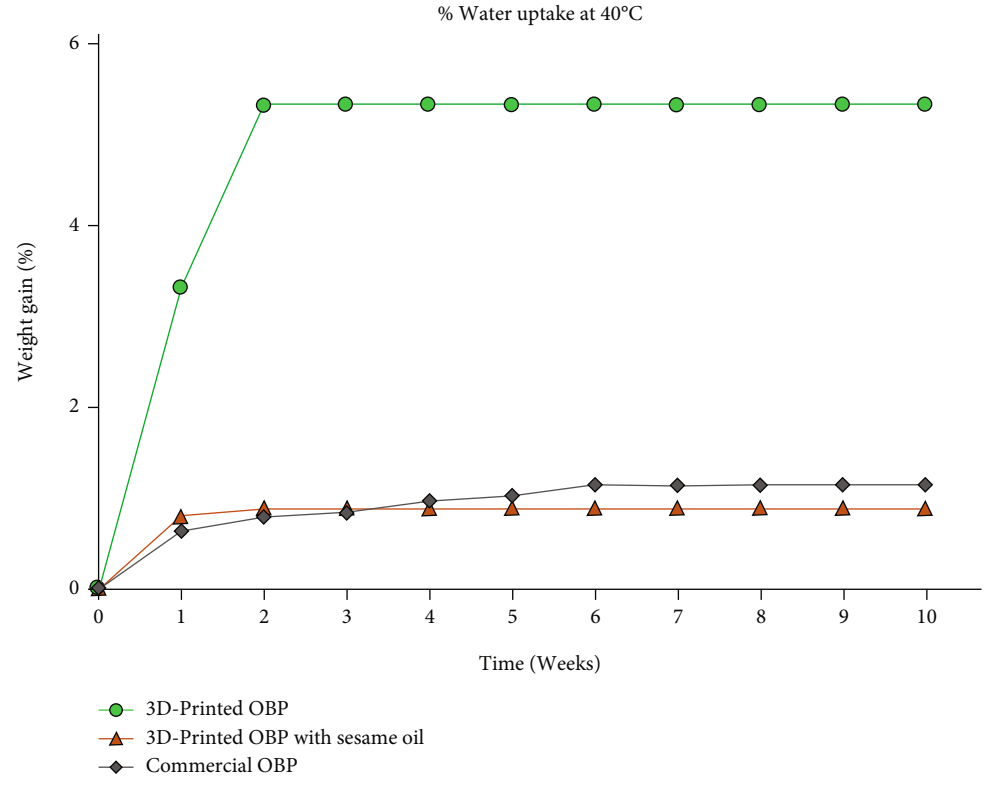

(b)

Figure 6: Continued.

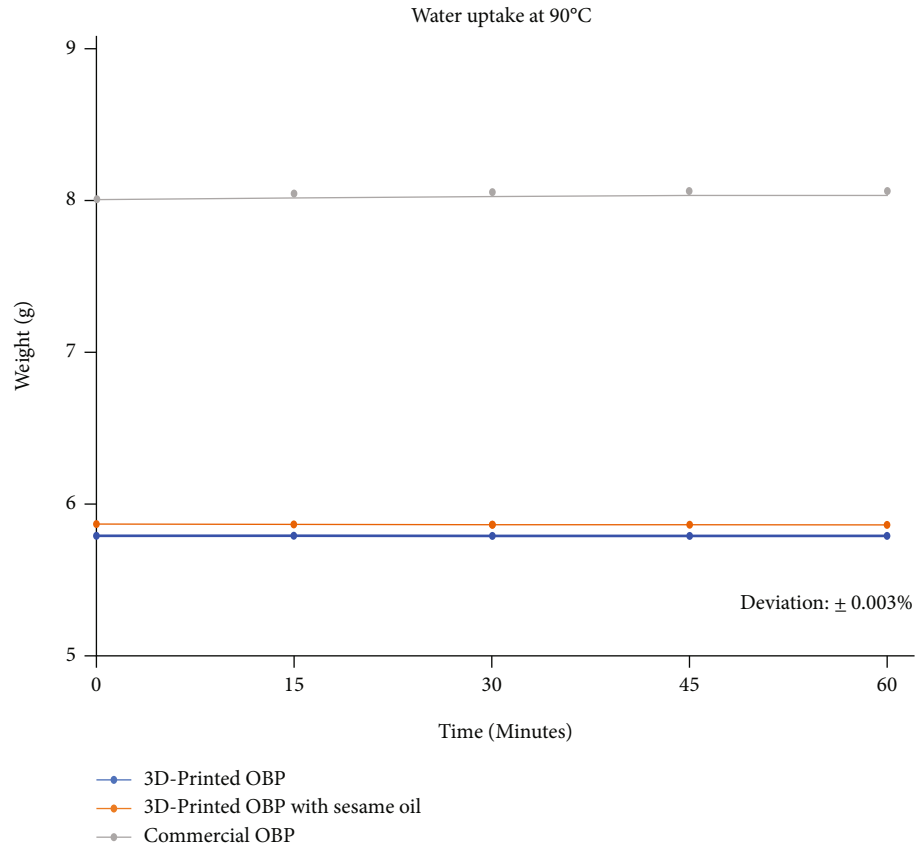

(c)

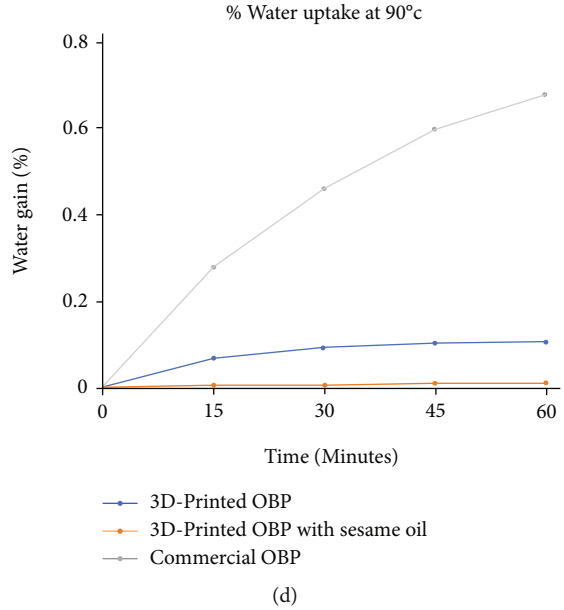

(d)

Figure 6: Water uptake capacity of the OBPs at (a) 40°C and (c) 90°C and percent water uptake by the OBPs at (b) 40°C and (d) 90°C.

densely packed and was in the process of conversion to its solid form "ice." Also, the motion of the molecules was slow enough to move into the structures of the OBPs.

The effect of pH, for values 5 and 9, on the water uptake capacity at temperatures of 0°C, 40°C, and 90°C was also found to be negligible. Therefore, the results given above for three different temperatures at pH 7 are similar to the results obtained for pH values 5 and 9. It is to be further noted that during the analyses of water uptakes under different temperature and pH conditions, the dimensional stability of both the commercial and fabricated OBPs remained unchanged, i.e., there were no noticeable changes in the x

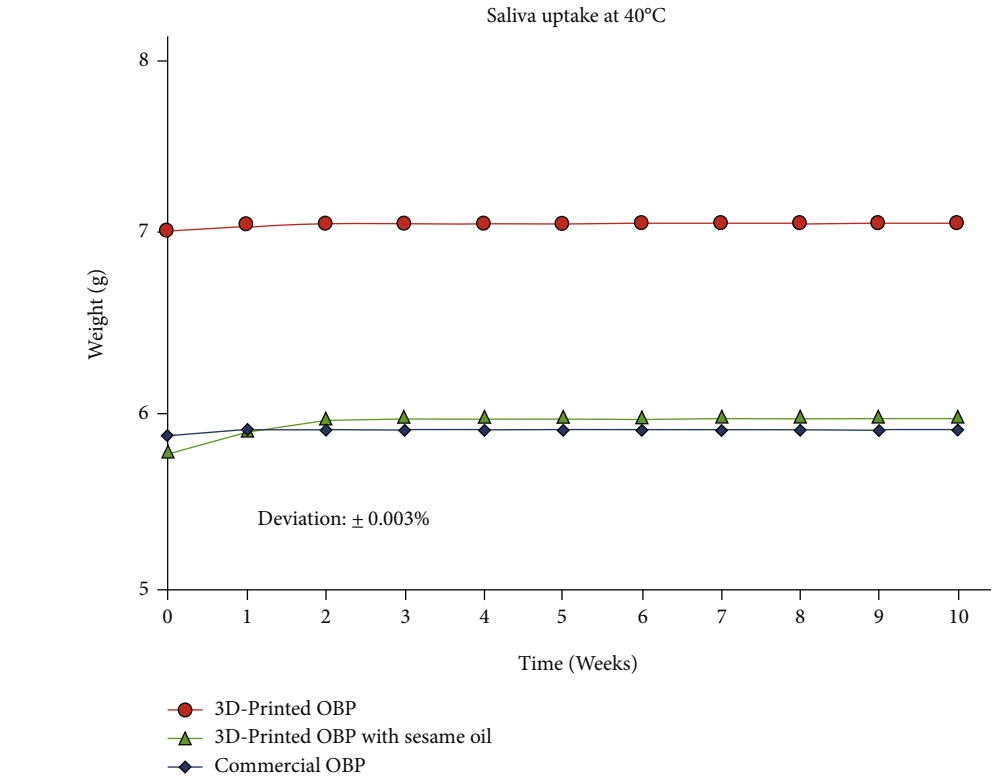

(a)

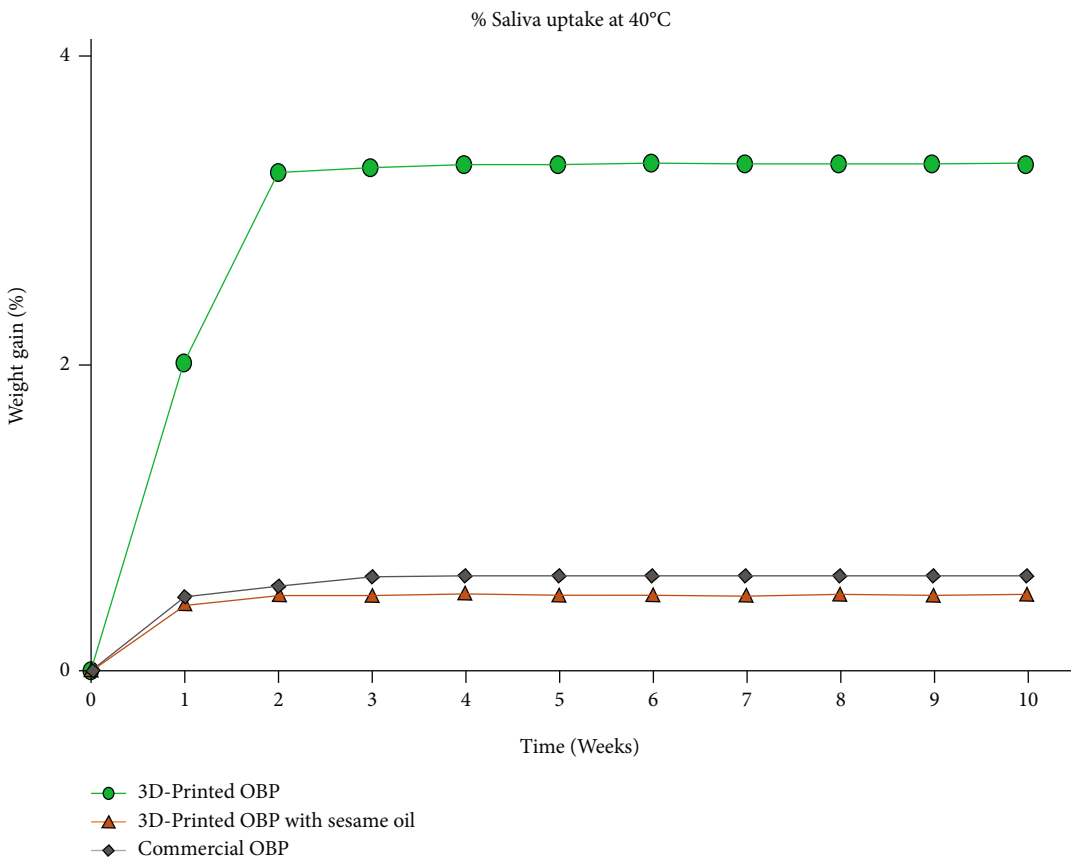

(b)

Figure 7: Continued.

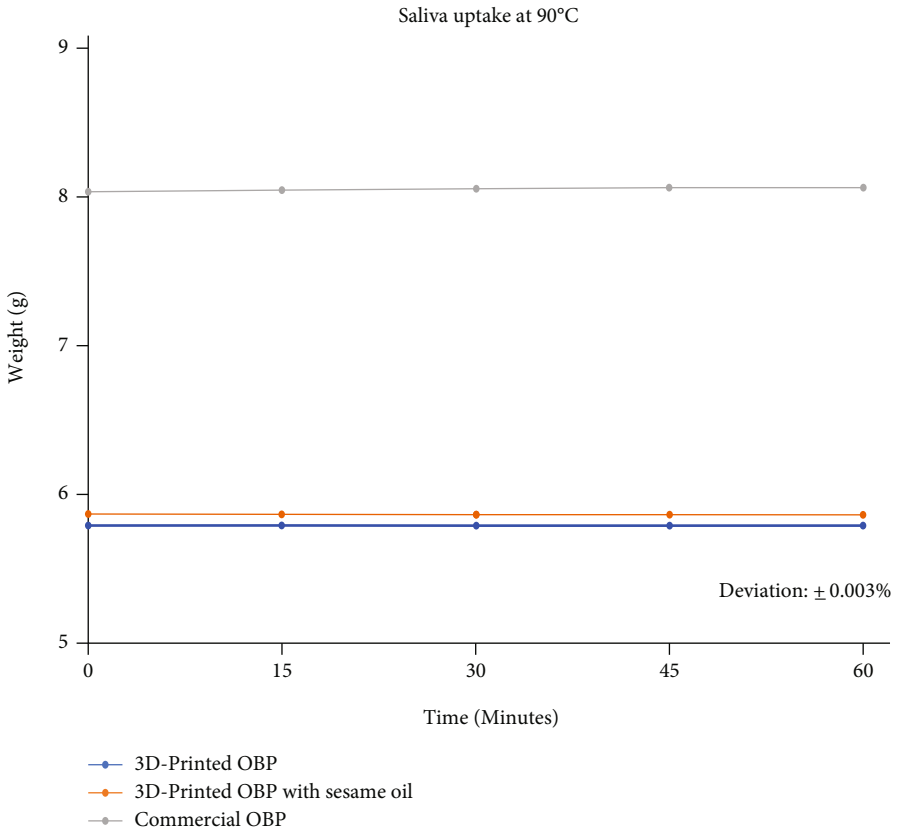

(c)

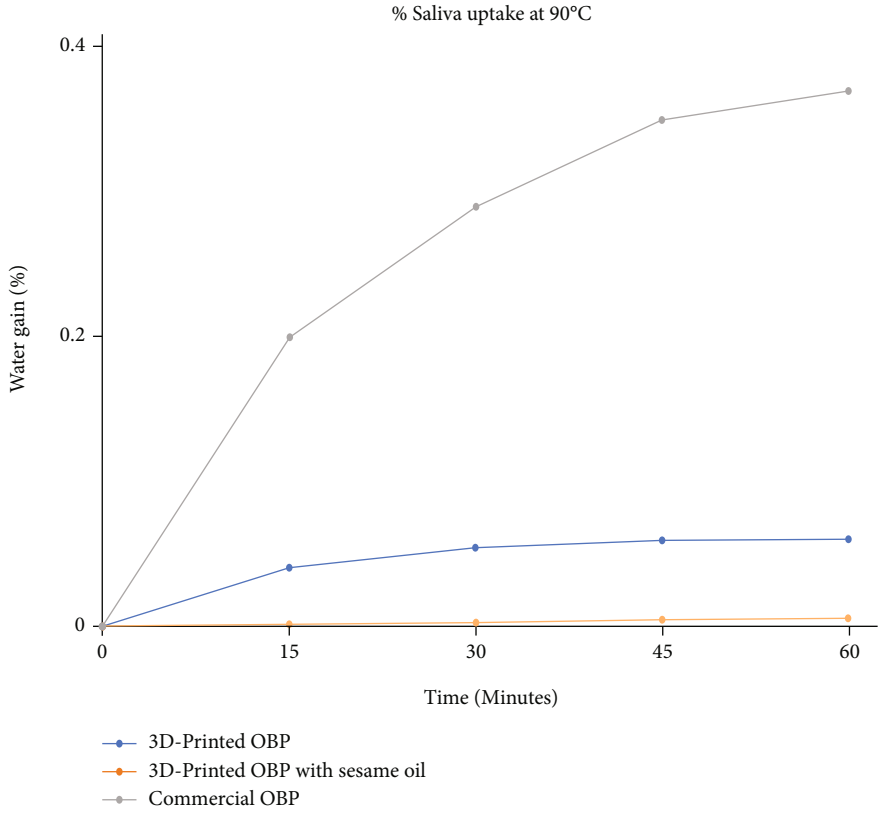

(d)

Figure 7: Saliva uptake capacity of the OBPs at (a) 40°C and (c) 90°C and percent saliva uptake by the OBPs at (b) 40°C and (d) 90°C.

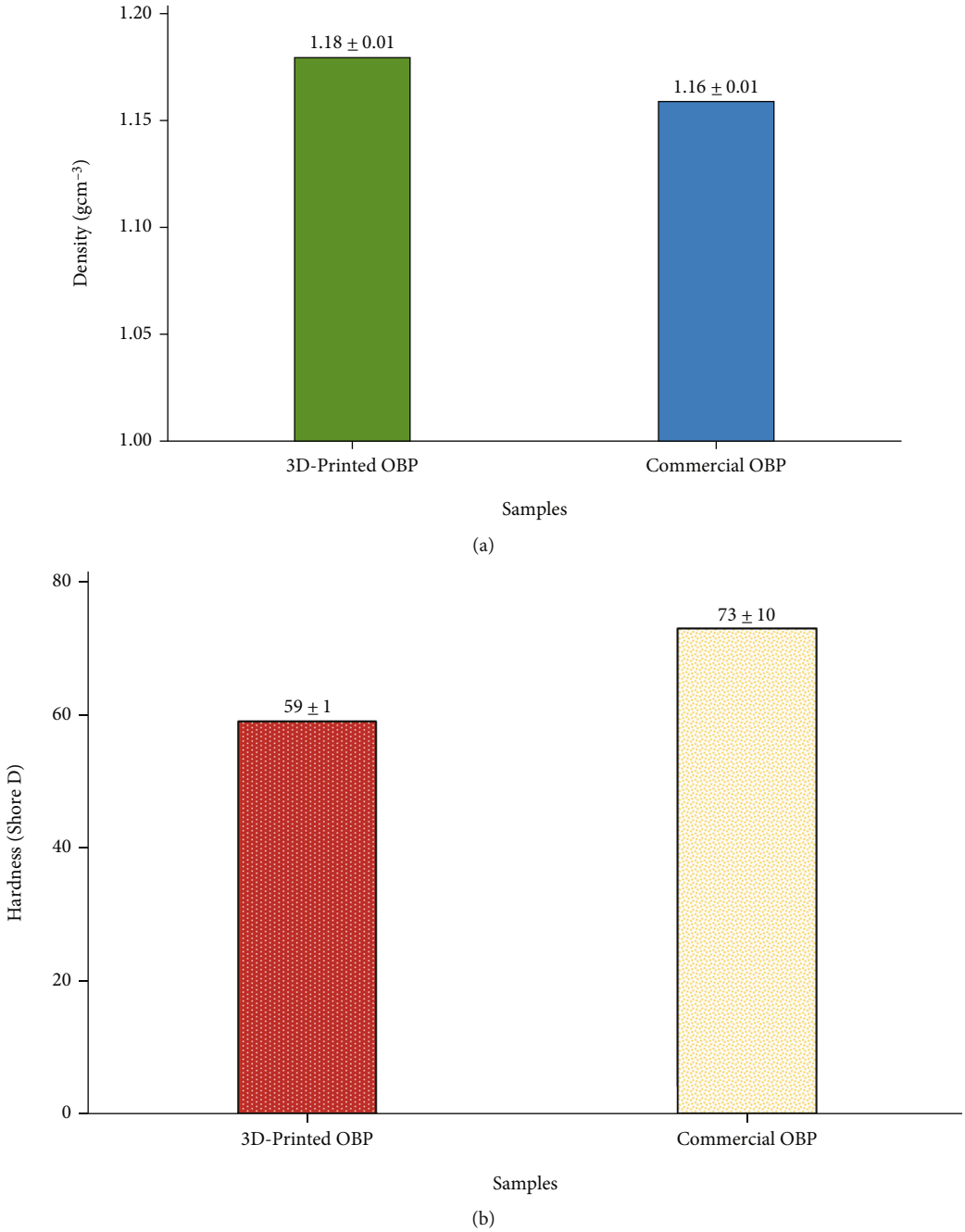

Figure 8: Comparative analysis of (a) the density of the developed OBP with the commercial OBP and (b) the Shore D hardness of the OBPs.

(length), y (width), and z (thickness) dimensions of the OBPs.

3.5. Analyses of Saliva Uptake and Dimensional Stability. Analyzing the uptake of artificial saliva shall provide a more realistic interpretation of the uptake behavior and dimensional stability of the OBPs. Keeping this in mind, the saliva uptake analyses were performed at three different temperatures, i.e., 0°C, 40°C, and 90°C, at a maintained pH value of 7. In addition, saliva uptake analyses at pH values of 5 and 9 were also carried out, using three different temperatures of 0°C, 40°C, and 90°C. In this respect, it has to be noted that artificial saliva is a mixture of a number of components apart from pure water. These are polysaccharides, sodium carboxymethylcellulose, sodium citrate, diglycerol, and artificial flavor. Therefore, it can be realized that owing to the larger molecular sizes of the constituents, compared to pure water, the uptake of saliva should be much lower compared to that observed with pure water [24].

In the analyses at 40°C, it was observed that although the saliva uptake trend was similar to that observed for the water uptakes (i.e., unmodified 3D printed PLA OBP > commercial OBP > oil-modified 3D printed PLA OBP), the actual uptake values for saliva were less than the values obtained for pure

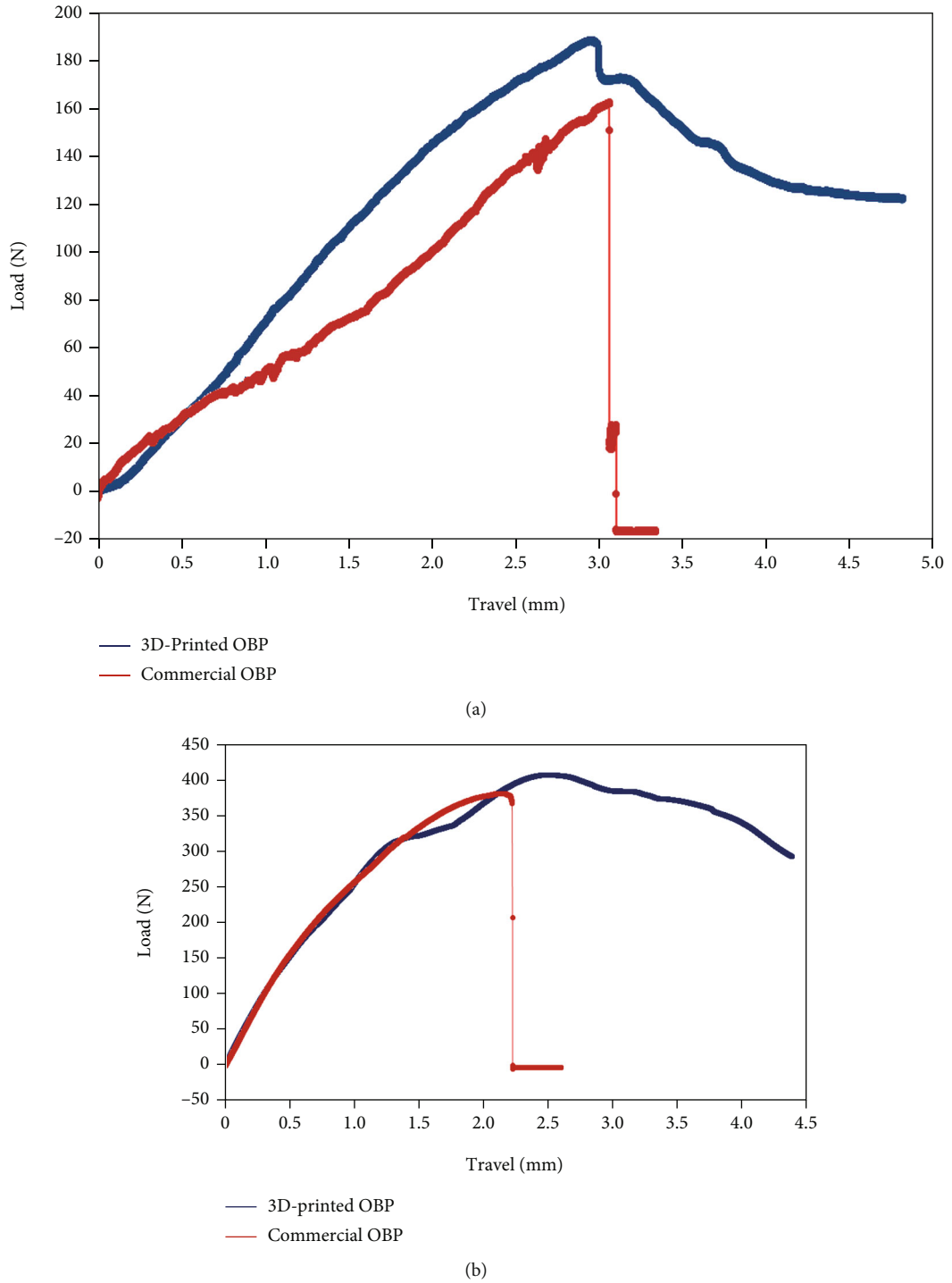

FIGURE 9: Comparative analysis of the maximum load bearing capacity of (a) the untreated 3D printed PLA and commercial OBPs and (b) the sesame oil-modified 3D printed PLA and commercial OBPs, after immersion in artificial saliva for 2 weeks. The standard deviation for both of these experiments has been found to be within ±2.5%.

water (Figures 7(a) and 7(b)). The obtained results are comparable to that observed by Łysik et al. [25] Similarly, in case of the saliva uptake analyses at 90°C, the pattern was found to be the same as observed for water uptake; however, the actual uptake values were much lower in case of the saliva uptakes (Figures 7(c) and 7(d)). Again, no noticeable uptakes were observed for analysis at 0°C as well as at pH values of 5 and 9. Also, no dimensional changes in the x, y, and z axes were found to occur.

3.6. Density Analyses in Water. As per literature, the density of PLA generally varies between 1.20 gcm^{-3} and 1.25 gcm^{-3} [26], while the density of PMMA is 1.19 gcm^{-3} [27]. However, in the present analysis, the density of the oil-modified

Table 1: Comparative analyses of tensile, flexural, and compressive strengths of unmodified PLA, oil-modified PLA, and literature reports on acrylic resins.

Properties	PLA	Oil-modified PLA	Literature reports on acrylic resins	Reference no.
Tensile strength (MPa)	52.3	59.7	48-62	31, 33
Flexural strength (MPa)	54.6	62.2	60-75	34
Compressive strength (MPa)	70.4	78.5	76	33

3D printed PLA OBP was observed to be 1.18 gcm^{-3} (Figure 8(a)). This lower density, compared to the literature value, can be attributed to the cumulative effect of the porous structure of the OBP, the presence of sesame oil (density: 0.92 gcm^{-3}) [28], and the presence of water (density: ~1 gcm^{-3}) within the pores of the OBP. On the other hand, the density of the commercial PMMA observed in this analysis (i.e., 1.16 gcm^{-3}) was slightly lower than that reported in the literature (i.e., 1.19 gcm^{-3}) (Figure 8(a)). This was the result of the presence of water (density: ~1 gcm^{-3}) within the structure of the PMMA OBP.

3.7. Shore D Hardness Analyses. Analysis of product hardness was carried out in order to ascertain the ease and comfort of wearing the developed plate, in comparison to the commercial plate. As can be seen from Figure 8(b), the Shore D hardness value measured for the developed PLA-based OBP was much lower compared to the commercial PMMA-based OBP. This is probably because of the higher porous structure of the PLA-based OBP, compared to the PMMA-based OBP. This result, which is comparable to that reported by Ansari and Kamil [29], signifies that the patients will feel more comfortable in wearing the PLA-based plate, compared to the commercial plate.

3.8. Maximum Load Bearing Capacity Analyses. During use, an OBP has to withstand certain amount of mechanical load that arises out of chewing and biting actions of teeth. The ability of the OBP to resist this load can be realized from its maximum load bearing capacity analysis. Therefore, this critical analysis was performed, first with the dry and unmodified 3D printed PLA OBP, followed by the oil-modified 3D printed PLA OBP after immersion in artificial saliva for 2 weeks. The results obtained were compared with dry and wet (after immersion in artificial saliva for 2 weeks) PMMA-based OBP, respectively. The period of 2 weeks was selected because from the saliva uptake analyses, it was realized that the uptakes took place for an average period of approximately 2 weeks.

Under dry conditions, the unmodified 3D printed PLA OBP was found to withstand a maximum load of ~190 N, following which the material showed signs of gradual failure (Figure 9(a)). However, in case of the commercial PMMA-based OBP, the maximum load bearing capacity was found to be ~160 N, followed by a catastrophic failure (Figure 9(a)). It should be noted here that catastrophic failure behavior is completely undesirable in a product. In this regard, PLA OBP, which showed a higher load bearing capacity and a gradual failure behavior, can be considered as a very superior alternative to its PMMA-based counterpart.

Figure 9(b) presents the maximum load bearing capacity analyses of oil-modified 3D printed PLA OBP and the commercial PMMA OBP, under wet conditions (i.e., after keeping the OBPs immersed in artificial saliva for 2 weeks). It was pleasing to note that there were significant enhancements in the maximum load bearing capacities of both the OBPs after they were immersed in saliva (Figure 9(b)). While the oil-modified 3D printed PLA OBP demonstrated a value of 410 N, the commercial PMMA-based OBP produced a value of 370 N. This overall enhancement of the maximum load bearing capacity under wet conditions can be attributed to the plasticizing effect of water (present in the saliva) for both the OBPs, as well as that of oil for the developed OBP. Nevertheless, the catastrophic failure behavior of the PMMA-based OBP was again realized, as against the gradual failure behavior of the developed OBP.

It should be noted here that the usual mastication force generated in human is between 70 N and 150 N [30]. However, this can reach up to a maximum of 500 N to 700 N in rare cases. Therefore, it can be safely said that the developed PLA-based OBP can perform its duty without the risk of failure under normal operation range. In fact, it shall function in a better manner than the commercial PMMA-based OBP.

3.9. Tensile, Flexural, and Compressive Strength Analyses. The tensile, flexural, and compressive strength analyses of the developed material were finally performed in order to ensure that it is capable enough for being fabricated into an OBP. It was found that the oil-modified PLA exhibited improved performance over the unmodified PLA (Table 1). These improvements can be attributed to the plasticizing effect of oil. In addition, the values observed for the oil-modified PLA were at par or better than that of the acrylic resins reported in the literature (Table 1) [31–34].

4. Conclusion

Herein, sesame oil (1 to 2 wt%)-incorporated 3D printed PLA OBPs have been fabricated and characterized as a potential alternative to conventional PMMA-based OBPs. The alternative OBPs demonstrated lighter weight, much higher product precision, and ease-of-fabrication and replication, as compared to the commercial OBPs. In addition, the 3D printed OBPs exhibited highly reduced water and saliva uptakes than the commercial OBPs at 40°C and 90°C, as well as negligible uptakes at 0°C. Also, effect of pH on the uptake values at different temperatures, as well as dimensional changes upon uptake as different temperature and pH values, was found to be insignificant. Moreover, the density and Shore D hardness of the alternative OBP was found to be slightly higher (i.e.,

$1.18 \pm 0.01\,gcm^{-3}$) and significantly lower (i.e., 59 ± 1), respectively, when compared with PMMA-based OBP (i.e., $1.16 \pm 0.01\,gcm^{-3}$ and 73 ± 10, respectively). Furthermore, the maximum load bearing capacity of the oil-incorporated PLA OBP was observed to be superior (exhibiting gradual failure) to the commercial OBP (exhibiting catastrophic failure), after treatment with saliva solution for 2 weeks. From the above results and discussion, it has been undoubtedly proven that 3D printed biodegradable-grade PLA, incorporated with minimal quantity of edible grade sesame oil, can perform as a suitable and tentatively biodegradable alternative to the commercial PMMA-based OBPs. However, further confirmations in terms of actual biocompatibility in human patients and biodegradability are essential before the actual effectiveness and suitability of the developed product can be claimed. Moreover, although very low material cost has been achieved in the developed product, the processing cost is still a bit high. These aspects have to be addressed before the developed PLA-based OBP can be declared fit for commercial exploitation.

Data Availability

The data presented in this study are available on request from the corresponding author. The data are not publicly available due to privacy based on patent application.

Additional Points

Patent. An Indian Patent has been applied for the work reported in this manuscript.

Conflicts of Interest

The authors declare no conflict of interest.

Authors' Contributions

K.D., N.N., and K.S. are responsible for the conceptualization; K.D. for the methodology and software; K.D., N.N., and K.S. for the validation; K.D., D.B., and A.V.H. for the formal analysis; N.N. for the resources; K.D. and D.B. for the data curation; K.D. for the writing—original draft preparation; K.D. and N.N. for the writing—review and editing; K.D. for the visualization; K.D. and K.S. for the supervision; and K.D., N.N., and K.S. for the project administration.

Supplementary Materials

The following supporting information can be downloaded at: http://www.mdpi.com/xxx/s1. Figure S1: structural defects, dimensional imperfections, and nonuniformity present in conventional PMMA-based OBPs. Figure S2: 3D scan image obtained from the conventional PMMA OBP and used for the 3D printing of the PLA OBP. *(Supplementary Materials)*

References

[1] Z. Raszewski, A. Nowakowska-Toporowska, D. Nowakowska, and W. Więckiewicz, "Update on acrylic resins used in dentistry," *Mini Reviews in Medicinal Chemistry*, vol. 21, no. 15, pp. 2130–2137, 2021.

[2] I. T. A. Peixoto, C. Enoki, I. Y. Ito, M. A. N. Matsumoto, and P. Nelson-Filho, "Evaluation of home disinfection protocols for acrylic baseplates of removable orthodontic appliances: a randomized clinical investigation," *American Journal of Orthodontics and Dentofacial Orthopedics*, vol. 140, no. 1, pp. 51–57, 2011.

[3] J. Brown and W. J. S. Kerr, "Light-curing acrylic resin as an orthodontic baseplate material," *Orthodontics*, vol. 29, pp. 508–512, 1998.

[4] F. C. R. Lessa, C. Enoki, I. Y. Ito, G. Faria, M. A. N. Matsumoto, and P. Nelson-Filho, "In-vivo evaluation of the bacterial contamination and disinfection of acrylic baseplates of removable orthodontic appliances," *American Journal of Orthodontics and Dentofacial Orthopedics*, vol. 131, no. 6, pp. 705.e11–705.e17, 2007.

[5] S. Thaweboon and B. Thaweboon, "*In vitro* study of *Streptococcus mutans* biofilm formation on vanillin-incorporated orthodontic PMMA resin," *Key Engineering Materials*, vol. 801, pp. 9–14, 2019.

[6] P. Thaitammayanon, C. Sirichompun, and C. Wiwatwarrapan, "Ultrasonic treatment reduced residual monomer in methyl methacrylate-based orthodontic base-plate materials," *Dental, Oral and Craniofacial Research*, vol. 4, pp. 1–5, 2018.

[7] W. Thummawanich, C. Wiwatwarrapan, and C. Sirichompun, "Effect of ultrasonic bath immersion on physical properties of an MMA-based orthodontic base-plate material," *Journal of Clinical and Diagnostic Research*, vol. 12, pp. ZC09–ZC12, 2018.

[8] H. M. Kopperud, I. S. Kleven, and H. Wellendorf, "Identification and quantification of leachable substances from polymer-based orthodontic base-plate materials," *European Journal of Orthodontics*, vol. 33, no. 1, pp. 26–31, 2011.

[9] P. Thaitammayanon, C. Sirichompun, and C. Wiwatwarrapan, "Comparison of residual monomer in the MMA-based orthodontic base-plate materials before and after water immersion," *Journal of Dentistry Chulalongkorn University*, vol. 38, pp. 67–74, 2015.

[10] R. E. Drumright, P. R. Gruber, and D. E. Henton, "Polylactic acid technology," *Advanced Materials*, vol. 12, no. 23, pp. 1841–1846, 2000.

[11] J. M. Anderson and M. S. Shive, "Biodegradation and biocompatibility of PLA and PLGA microspheres," *Advanced Drug Delivery Reviews*, vol. 64, pp. 72–82, 2012.

[12] X. Pang, X. Zhuang, Z. Tang, and X. Chen, "Polylactic acid (PLA): research, development and industrialization," *Biotechnology Journal*, vol. 5, no. 11, pp. 1125–1136, 2010.

[13] R. E. Conn, J. J. Kolstad, J. F. Borzelleca et al., "Safety assessment of polylactide (PLA) for use as a food-contact polymer," *Food and Chemical Toxicology*, vol. 33, no. 4, pp. 273–283, 1995.

[14] M. S. Singhvi, S. S. Zinjarde, and D. V. Gokhale, "Polylactic acid: synthesis and biomedical applications," *Journal of Applied Microbiology*, vol. 127, no. 6, pp. 1612–1626, 2019.

[15] G. Li, M. Zhao, F. Xu et al., "Synthesis and biological application of polylactic acid," *Molecules*, vol. 25, no. 21, Article ID 5023, 2020.

[16] N. Singh and G. Singh, "Advances in polymers for bio-additive manufacturing: a state of art review," *Journal of Manufacturing Processes*, vol. 72, pp. 439–457, 2021.

[17] R. Singh, H. Singh, I. Farina, F. Colangelo, and F. Fraternali, "On the additive manufacturing of an energy storage device from recycled material," *Composites Part B: Engineering*, vol. 156, pp. 259–265, 2019.

[18] T. Casalini, F. Rossi, A. Castrovinci, and G. Perale, "A perspective on polylactic acid-based polymers use for nanoparticles synthesis and applications," *Frontiers in Bioengineering and Biotechnology*, vol. 7, p. 259, 2019.

[19] S. K. Singh, P. Anthony, and A. Chowdhury, "High molecular weight poly(lactic acid) synthesized with apposite catalytic combination and longer time," *Oriental Journal of Chemistry*, vol. 34, no. 4, pp. 1984–1990, 2018.

[20] P. Gómez-Contreras, M. Contreras-Camacho, F. Avalos-Belmontes, S. Collazo-Bigliardi, and R. Ortega-Toro, "Physicochemical properties of composite materials based on thermoplastic yam starch and polylactic acid improved with the addition of epoxidized sesame oil," *Journal of Polymers and the Environment*, vol. 29, no. 10, pp. 3324–3334, 2021.

[21] A. M. Pandele, A. Constantinescu, I. C. Radu, F. Miculescu, S. I. Voicu, and L. T. Ciocan, "Synthesis and characterization of PLA-micro-structured hydroxyapatite composite films," *Materials*, vol. 13, no. 2, p. 274, 2020.

[22] M. D. G. Neves and R. J. Poppi, "Monitoring of adulteration and purity in coconut oil using Raman spectroscopy and multivariate curve resolution," *Food Analytical Methods*, vol. 11, no. 7, pp. 1897–1905, 2018.

[23] J. V. Ecker, A. Haider, I. Burzic, A. Huber, G. Eder, and S. Hild, "Mechanical properties and water absorption behaviour of PLA and PLA/wood composites prepared by 3D printing and injection moulding," *Rapid Prototyping Journal*, vol. 25, no. 4, pp. 672–678, 2019.

[24] S. Gopalakrishnan, I. Raj, A. T. Mathew et al., "Development of oral-fluid-impervious and fracture-resistant silver–poly(-methyl methacrylate) nanoformulations for intra-oral/extra-oral rehabilitation," *Journal of Applied Polymer Science*, vol. 136, no. 26, Article ID 47669, 2019.

[25] D. Łysik, J. Mystkowska, G. Markiewicz, P. Deptuła, and R. Bucki, "The influence of mucin-based artificial saliva on properties of polycaprolactone and polylactide," *Polymers*, vol. 11, no. 11, Article ID 1880, 2019.

[26] H. K. Dave, S. R. Rajpurohit, N. H. Patadiya et al., "Compressive strength of PLA based scaffolds: effect of layer height, infill density and print speed," *international journal of modern manufacturing technologies*, vol. XI, pp. 21–27, 2019.

[27] S.-K. Yeh, N. M. Demewoz, and V. Kurniawan, "Controlling the structure and density of PMMA bimodal nanocellular foam by blending different molecular weights," *Polymer Testing*, vol. 93, article 107004, 2021.

[28] S. V. Sujith, A. K. Solanki, and R. S. Mulik, "Experimental investigations on viscosity and density of eco-friendly MoS_2-sesame oil nano-lubricants and its influence on pumping power," *Nanotechnology*, vol. 32, no. 36, article 365702, 2021.

[29] A. A. Ansari and M. Kamil, "Izod impact and hardness properties of 3D printed lightweight CF-reinforced PLA composites using design of experiment," *International Journal of Lightweight Materials and Manufacture*, vol. 5, no. 3, pp. 369–383, 2022.

[30] C. Scully, *Oxford Handbook of Applied Dental Sciences*, Oxford University Press, New York, 2002.

[31] P. Spasojevic, M. Zrilic, V. Panic, D. Stamenkovic, S. Seslija, and S. Velickovic, "The mechanical properties of a poly(-methyl methacrylate) denture base material modified with dimethyl itaconate and di-*n*-butyl itaconate," *International Journal of Polymer Science*, vol. 2015, Article ID 561012, 9 pages, 2015.

[32] M. S. Zafar, "Prosthodontic applications of polymethyl methacrylate (PMMA): an update," *Polymers*, vol. 12, no. 10, Article ID 2299, 2020.

[33] R. K. Alla, K. N. R. Swamy, R. Vyas, and A. Konakanchi, "Conventional and contemporary polymers for the fabrication of denture prosthesis: part I–overview, composition and properties," *International Journal of Applied Dental Sciences*, vol. 1, pp. 82–89, 2015.

[34] M. Chhabra, M. N. Kumar, K. N. Raghavendra Swamy, and H. M. Thippeswamy, "Flexural strength and impact strength of heat-cured acrylic and 3D printed denture base resins- a comparative in vitro study," *Journal of Oral Biology and Craniofacial Research*, vol. 12, no. 1, pp. 1–3, 2022.